

Radio Frequency Plasma Processing to Produce Chromium Sputter Targets

M. Müller, R.B. Heimann, F. Gitzhofer, M.I. Boulos, and K. Schwarz

(Submitted 17 January 2000)

Production of thick chromium layers on copper substrates used for sputter targets provides a number of technological challenges. These challenges were addressed using radio frequency (RF) plasma spray technology. The efforts were focused on several objectives. The coatings should be as dense as possible with residual stresses low enough to avoid strong substrate bending and to prevent adhesive and/or cohesive failure of the coating. In addition, the deposition efficiency should be maximized.

Different parameters were varied to find the optimum spraying conditions. Two different powder grain sizes, $-90 + 45 \mu\text{m}$ and $-63 + 20 \mu\text{m}$, were used. First, a spheroidization study was performed to select the most suitable chamber pressure, the optimum plasma power, and a reasonable range of the powder feed rate. During deposition of the coatings, the powder feed rate, the spray distance, the substrate roughness, and the substrate cooling mode were optimized. The substrates were noncooled, gas cooled, or directly water cooled, respectively. The water-cooled samples showed no substrate bending; however, the thermal stresses occurring were strong enough to cause coating failure in adhesion or cohesion. Noncooled samples showed the best adhesion properties, while substrate bending could be kept within acceptable limits.

Keywords chromium target, copper substrate, powder spheroidization, RF plasma spraying, tensile adhesion

1. Introduction

Today physical vapor deposition (PVD) technology is widely used to produce thin coatings for many applications, including magnetic tapes, resistors, semiconductors, ultra violet (UV) and infrared (IR) filters, reflection coatings, wear and/or corrosion resistant coatings, mirror coatings, and decorative coatings. Customarily, the PVD sputter targets have been manufactured by traditional metallurgical processes such as powder consolidation or liquid metal casting. Recently, DC vacuum plasma spraying was employed as an alternative technology to produce Cr sputter targets.^[1,2,3]

In this study, we attempt to spray chromium coatings about 6 mm thick onto copper substrates using an RF inductively coupled plasma. Copper is a substrate material well suited for targets because of its high electrical and thermal conductivities.

It was the purpose of this work to find the optimum deposition conditions for the major quality features of the targets by variation of six parameters: powder grain size, substrate roughness, substrate cooling mode, chamber pressure, spray distance, and powder feed rate. The adhesion strength must be high enough to make the target withstand the final machining and to ensure the required electrical contact within the target. However, strong residual stresses are caused by the large difference of the

coefficients of thermal expansion of the two metals: Cu $16.5 \times 10^{-6} \text{ K}^{-1}$ and Cr $6 \times 10^{-6} \text{ K}^{-1}$ (at 0°C).^[4] These stresses must be minimized since they can give rise to delamination of the coating and to strong substrate bending.^[5] The density of the coating must be maximized to obtain low contamination and a long service life of the target. The deposition efficiency is an important economical aspect of the process and hence should be as high as possible.

2. Experimental Procedure

2.1 Spheroidization Study

All experiments were performed with the RF 50 installation at the Centre de Recherche en Technologie des Plasmas (CRTP) at the University of Sherbrooke (Sherbrooke, QC, Canada). The system was run with an oscillator frequency of about 3 MHz. The plasma was generated by a PL 50 plasma torch from TEKNA Plasma Systems Inc. (Sherbrooke). A standard gas mixture of 40 slm (standard liters per minute) argon (central gas), 90/9 slm argon/hydrogen (sheath gas), and 4 slm argon (powder carrier gas) was applied for both the spheroidization and the deposition studies.

The spheroidization study was performed to gain knowledge of the combination of the parameters (1) chamber pressure, (2) plasma power, (3) powder feed rate, and (4) powder grain size that will result in a maximum percentage of spheroidized powder and a minimum powder loss through vaporization.

The optimum parameter combination will cause all particles to be heated above their melting points (1860°C)^[4] without reaching and exceeding their boiling points (2670°C at 0.1 MPa,^[4]). However, this ideal situation is unattainable because the different particle sizes require widely varying amounts of energy for melting. Crushed chromium powders of two different grain sizes, $-63 + 20 \mu\text{m}$ and $-90 + 45 \mu\text{m}$ were used for the spheroidization study as well as for the deposition experiments.

M. Müller, German Aerospace Center (DLR), Institute for Technical Thermodynamics, Stuttgart, Germany; R.B. Heimann, Department of Mineralogy, Freiberg University of Mining and Technology, Freiberg, Germany; F. Gitzhofer and M.I. Boulos, Department of Chemical Engineering, University of Sherbrooke, Sherbrooke, QC, Canada; and K. Schwarz, Freiburger Nichteisen-Metall GmbH, Freiberg, Germany. Contact e-mail: matthias.mueller@dlr.de.

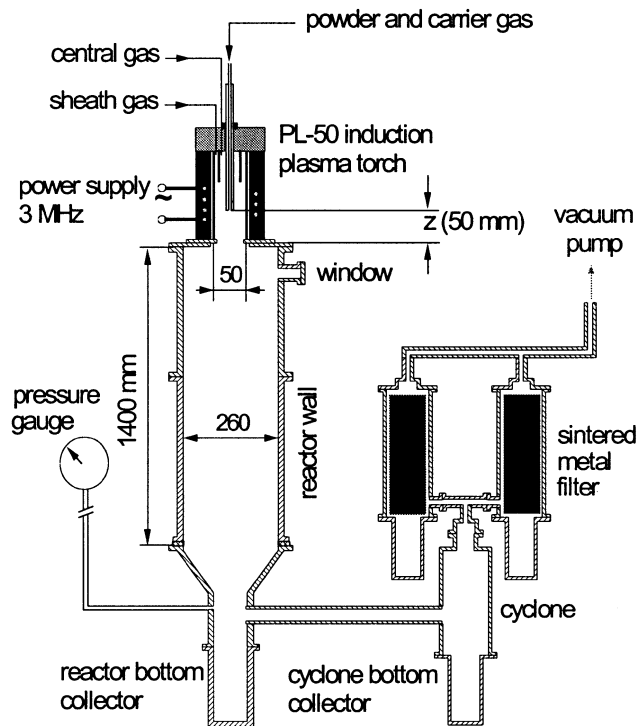
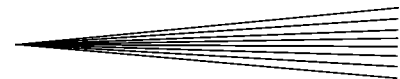


Fig. 1 Schematic drawing of the setup for the spheroidization experiments

Spherical chromium grains of 50 and 100 μm diameter require 764.6 and 6116.6 μJ , respectively. A sketch of the reactor used for the spheroidization study is shown in Fig. 1. Several series of parameter variations were performed during the spheroidization experiments (Table 1). The plate power was set to a constant value of about 42 kW, close to the upper limit of the system.

2.2 Coating Deposition

Substrate Preparation. Copper plates of 160 \times 100 mm² size and a thickness of either 5 or 8 mm were used as substrates. Since the influence of the substrate surface area on the adhesion strength was of interest, the substrate roughness was varied on three levels: (1) a sand-blasted surface only (“sandblast pattern”), (2) mechanical roughening with an endless spiral groove and subsequent sandblasting (“spiral pattern”), and (3) mechanical roughening with two orthogonal groove systems and subsequent sandblasting (“diamond pattern”).

Spray Conditions. According to the results of the spheroidization study (Section 3.1 and Table 1), the chamber pressure was set to 66 kPa for the $-90 + 45 \mu\text{m}$ powder and to 33 kPa for the $-63 + 20 \mu\text{m}$ powder. The powder feed rate was varied between 20 and 100 g/min. The spray distances were between 180 and 280 mm. The plate power was kept at about 42 kW. The substrates were moved along their 160 mm sides with 24 traverses per minute.

Substrate Cooling. The substrate temperature was expected to have a large influence on the adhesion strength. The temperature of the substrate should be high enough to obtain optimum adhesion, even if there is no metallurgical bonding to be expected between the two metals, as discussed below (“Mi-

Table 1 Parameter variations during the spheroidization experiments

Powder grain size (μm)	Chamber pressure (kPa)	Powder feed rate (g/min)
$-90 + 45$	66	20, 40, 60, 80, 120, 160
$-90 + 45$	33	33, 90
$-63 + 20$	66	20, 40, 60, 80
$-63 + 20$	33	26, 60, 74

crostructure” subsection). On the other hand, if the substrate is not cooled very efficiently, there is a large difference in the thermal expansion between coating and substrate. A high substrate temperature during spraying resulted in a strong shrinkage during cooling, and associated high residual stresses caused a strong bending of the substrate, leading eventually to coating delamination.^[5] Therefore, the substrate temperature should be kept as low as possible.

Both temperature extremes were tested, *i.e.*, a noncooled and a directly water-cooled substrate. All noncooled substrates were 8 mm thick. The directly water-cooled substrates (5 mm thick) were fixed to a holding jig, which allowed a uniform cooling of almost the entire back of the substrates by a water flow rate of 7 liters/min. Two experiments were performed with direct gas cooling (argon, gas flow rate 120 slm). The gas-cooled substrates were 8 mm thick.

2.3 Tensile Adhesion Test

Tensile adhesion tests of plasma-sprayed coatings, *e.g.*, ASTM C633^[6] and EN 582:1993,^[7] require the manufacture of cylindrical substrates of 1 in. diameter. During spraying of coatings onto such small specimens, only low stresses will occur. These stresses are difficult to compare to the stress conditions in much larger workpieces, particularly for layers of several millimeters thickness. Therefore, the substrate dimensions were 160 \times 100 \times 8 mm³ and 160 \times 100 \times 5 mm³, respectively, in order to investigate samples closer to the conditions of the target production. Two tensile test specimens of 1 in. diameter were machined from each as-sprayed sample by spark erosion. Both cylinder faces were plane polished and glued to steel plugs with Scotch-Weld Brand Epoxy Adhesive 2214 Hi-Density (3M Inc., St. Paul, MN) (Fig. 2). The specimens were aligned in an Instron test installation and then pulled apart according to the ASTM (Instron Corp., Canton MA) C633 standard conditions.^[6]

Sample Preparation and Evaluation

After machining of the tensile test cylinder samples, the target plates were cut for metallographic preparation. Polished cross sections were prepared to evaluate, by optical microscopy, the porosity and the processes presumably occurring at the interface, *e.g.*, possible formation of intermetallic compounds or alloys. The porosity was measured using the image analysis software KS 300 from Kontron Elektronik (München, Germany). Macrohardness measurements were also performed at the polished cross sections using a Brinell indenter with a load of 613.1 N.

Eventually, the cross sections were electrolytically etched in

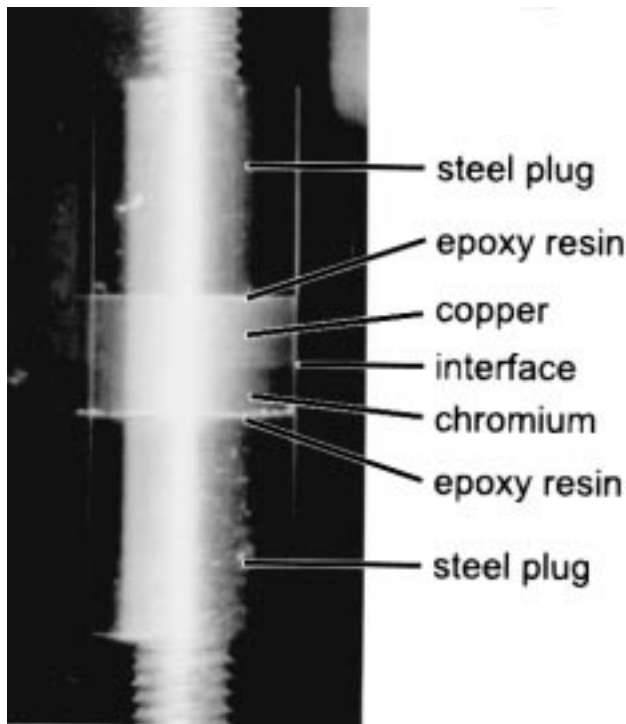


Fig. 2 Tensile test sample arrangement

20% oxalic acid to reveal the splat shape and to evaluate the degree of melting of the particles.

3. Results and Discussion

3.1 Spheroidization Study

Figure 3(a) to (f) show scanning electron microscopy (SEM) ((a), starting powder) and optical micrographs ((b) to (f), spheroidized particles) of powders subjected to varying conditions. At high chamber pressure (66 kPa), the coarse powder ($-90 + 45 \mu\text{m}$) was almost completely spheroidized (98%) up to a powder feed rate of 80 g/min (Fig. 3b). On increasing the feed rate to 120 g/min, the spheroidization efficiency decreased to a few percent (Fig. 3c). This tendency was confirmed by the results obtained with feed rates of 20, 60, and 160 g/min. At low pressure (33 kPa), the spheroidization behavior of the coarse powder is much less homogeneous. While there are only a few percent of non-molten particles, the sizes of the spheroids differ considerably, independent of the powder feed rate. Figure 3(d) shows an example of a powder obtained with a feed rate of 90 g/min with a spheroidization efficiency of about 85%.

In contrast to this, the finer powder ($-63 + 20 \mu\text{m}$) shows a homogeneous spheroidization behavior at low working pressure (33 kPa). At a feed rate of 74 g/min, about 90% of the particles were spheroidized (Fig. 3e). Deviating from the results obtained with the coarser powder, at higher pressure (66 kPa), the finer powder was poorly spheroidized, about 50% for the entire range of the powder feed rate (Fig. 3f).

It was not an objective of this study to find the reason for the completely different spheroidization behavior of the different

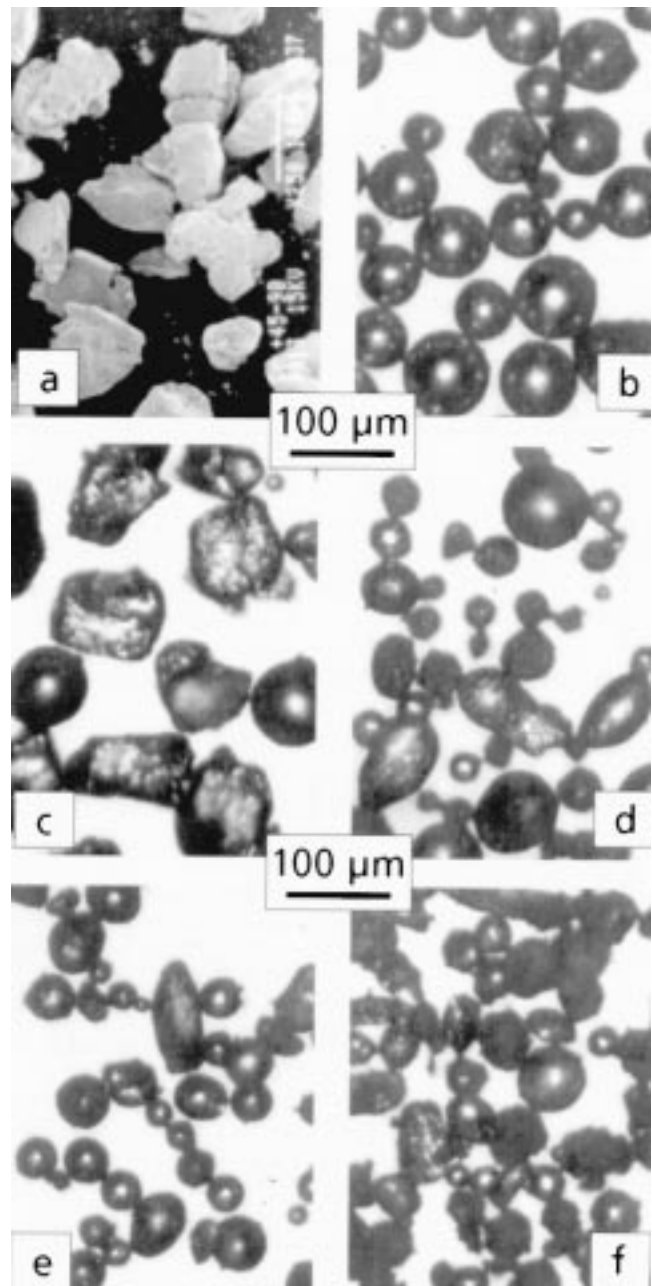


Fig. 3 (a) SEM and (b) to (f) optical micrographs of the starting powder $-90 + 45 \mu\text{m}$ (a) and powders collected in the reactor bottom (b) to (f). For an explanation, see the text

powder grain sizes. The main objective, and hence the major result, of the spheroidization study was the establishment of a parameter set for the deposition experiments. This parameter combination was given above in the “Spray Conditions” section.

3.2 Target Material Deposition

Deposition Efficiency. The deposition efficiency was found to be mainly a function of the spray distance and the powder feed rate for a given powder grain size. The deposition effi-

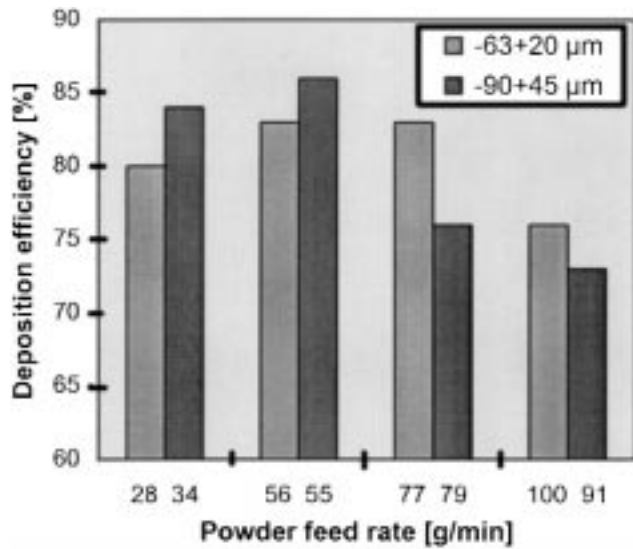


Fig. 4 Dependence of the deposition efficiency on the powder feed rate and the powder grain size

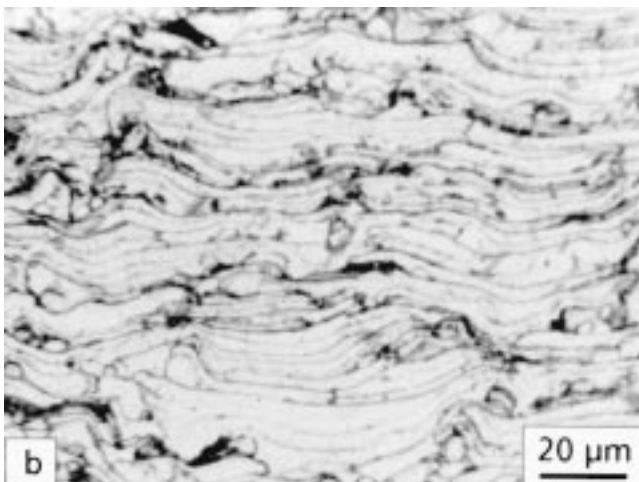
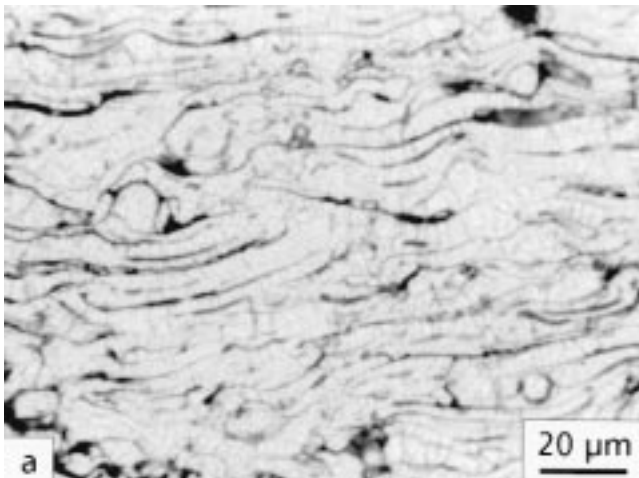


Fig. 5 Optical micrographs of etched cross sections of coatings sprayed under the following conditions: powder $-63 + 20 \mu\text{m}$, plate power 42 kW, spray distance 220 mm, powder feed rate 24 g/min, (a) direct water cooling and (b) gas cooling. Porosity about 3%

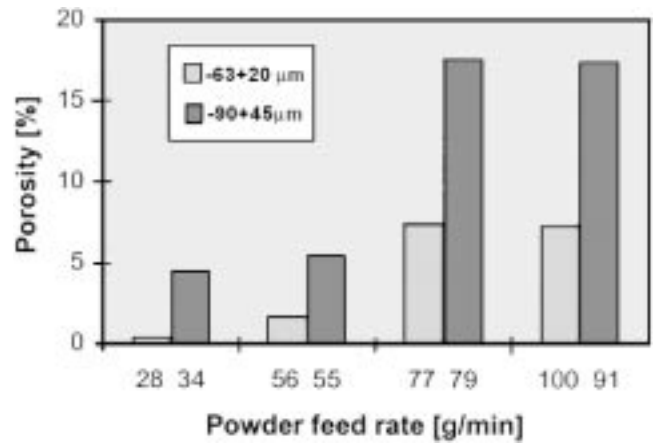


Fig. 6 Coating porosity as a function of the powder feed rate and the powder grain size

ciency could be maximized in the powder feed rate range of 50 to 80 g/min using the $-63 + 20 \mu\text{m}$ powder. Applying the coarser powder, a similar tendency was observed for an optimum feed rate of about 50 g/min (Fig. 4). A low feed rate resulted in an increased loss of material by vaporization, while too high a feed rate prevented complete melting of all particles fed into the plasma; hence, the nonmolten material will rebound from the substrate during spraying.

Spray distances of 220 mm for the $-63 + 20 \mu\text{m}$ powder and 180 mm for the $-90 + 45 \mu\text{m}$ powder, respectively, were found to yield the best deposition efficiencies of up to 88%. This, of course, is correlated to the chamber pressure that was twice as high when processing the coarser powder.

Not shown here is the slight decrease of the deposition efficiency observed for directly water-cooled substrates. This effect could be explained with the rebounding of the first particles impinging at the cold substrate.

Microstructure. Thick deposits show the typical layered structure of thermally sprayed coatings (Fig. 5). The porosity increased with increasing powder feed rate (Fig. 6). Porosities of less than 1% were found for coatings deposited onto noncooled substrates using the $-63 + 20 \mu\text{m}$ powder at a low feed rate of 28 g/min. Increasing the powder feed rate to 56 g/min yielded coatings with a porosity as low as 2%. A further increase of the feed rate to beyond 77 g/min resulted in a coating porosity of 7%.

The results obtained with the $-90 + 45 \mu\text{m}$ powder obey the same tendency, however, with greater overall porosity values. A feed rate of 55 g/min resulted in a porosity of about 6%; a further increase to 79 g/min yielded 17.5% porosity.

An optimum spray distance with regard to the porosity was achieved at 220 mm for the finer powder. The coarser powder was best processed with a distance of 180 mm, as already described above. The porosity values are roughly inversely proportional to the macro (Brinell) hardness values, as indicated in Fig. 7.

An effect of the substrate cooling mode on the porosity could also be observed. Using the finer powder, the porosity increased from 0.4% for the noncooled sample to 4.5% (gas-cooled sample) to 5.5% (water-cooled sample). Apparently, a particle im-

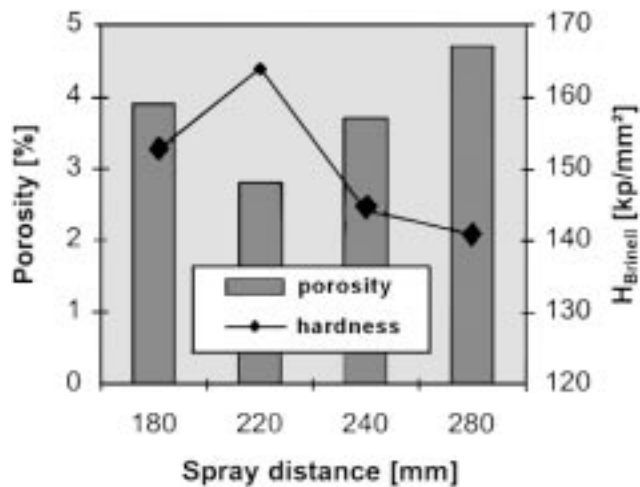


Fig. 7 Coating porosity and macrohardness as functions of the spray distance. Error bars were not given for simplicity. Directly water-cooled substrates. For other spray parameters, see the text

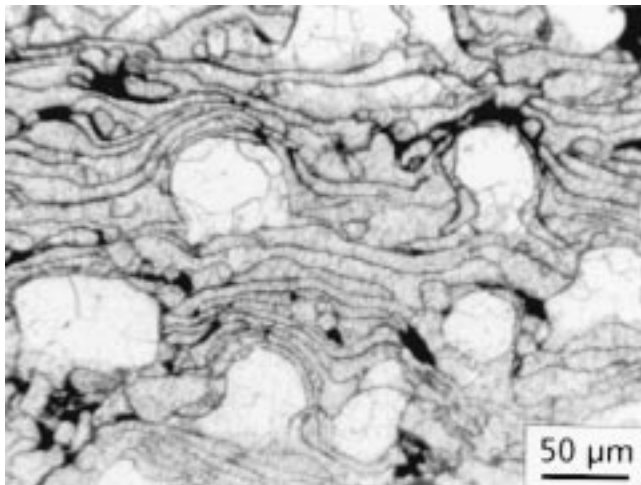


Fig. 8 Optical micrograph of an etched coating cross section. Porosity 5.9%

pinging at a hot surface flattens much wider and hence provides less space for pores.

Figure 8 reveals the ambiguity of the results of the spheroidization study. From the spheroidization experiments, one can conclude that a powder feed rate of up to 80 g/min for the $-90 + 45 \mu\text{m}$ powder resulted in almost complete melting of the particles (Fig. 3b). However, some particles showed melting of the outer surface only, with the core remaining solid already at a feed rate of 55% (Fig. 8). Under those conditions, only single nonmolten grains impinge at the substrate and can therefore be surrounded by liquid splats; hence, the porosity is just slightly increased to 5.9%. A further increase of the feed rate to 79 g/min resulted in a large coating porosity of about 17.5%.

Overheating of the substrate resulted in a partial melting of the copper plates. Obviously, this happened after the deposition of the first chromium layers, as indicated by the maintenance of the planar interface of the chromium deposit, while the copper

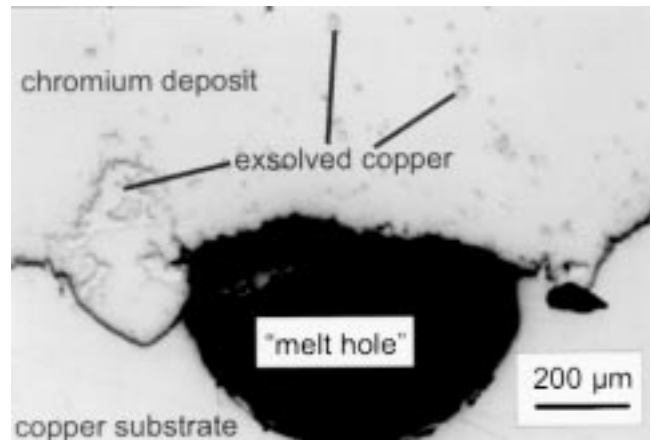


Fig. 9 Optical micrograph of a polished cross section revealing the absence of an intermetallic compound, but instead grains and lenses of exsolved copper in a chromium matrix

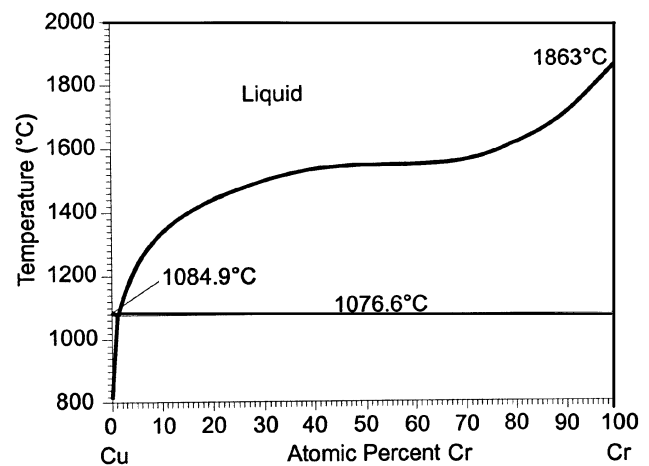


Fig. 10 Phase diagram Cr-Cu^[11]

shows holes from escaped molten material (Fig. 9). The molten copper diffused into the chromium but was later exsolved during the cooling process in response to the nonmiscibility of the two metals at low temperature. This behavior can be explained with literature data. Copper crystallizes in an fcc structure, while chromium crystallizes in a bcc structure. Because of the incommensurability of the structures, the metals are practically immiscible and do not form alloys or chemical compounds (Fig. 10.^[8-11])

Adhesion Strength. The values of the adhesion strength of the chromium deposits to the copper substrates emphasize the importance of an as large as possible substrate surface area. The direct water cooling of only sand-blasted substrates resulted in an immediate delamination of the deposit, while the machined and sand-blasted substrates provide many more anchor points and hence an increased though still low adhesion strength (Fig. 11). The comparison of the different substrate surface preparation methods applied to noncooled samples yielded the same tendency but with much higher adhesion strength values.

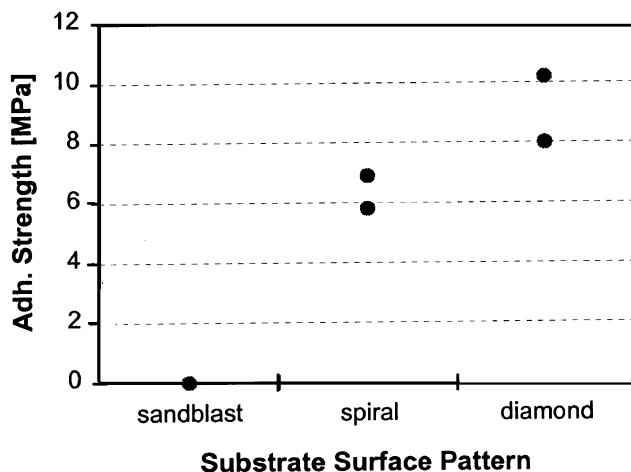


Fig. 11 Adhesion strength as a function of the substrate preparation technique of directly water-cooled samples

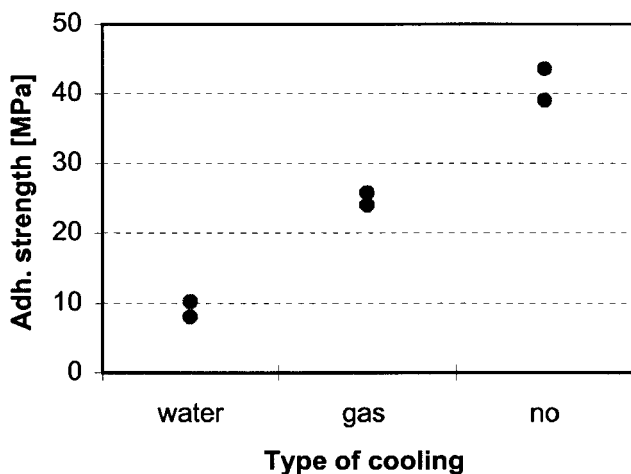


Fig. 12 Adhesion strength as a function of the cooling mode. Substrate preparation—water and gas cooled: diamond pattern + sandblasting; noncooled: sandblasted only

The adhesion strength is furthermore strongly dependent on the cooling mode of the substrate (Fig. 12). Adhesion strengths exceeding 40 MPa were even observed on a noncooled substrate that was only sandblasted. The failure occurring in those specimens was not adhesive but cohesive.

Depending on the substrate surface preparation, the failure that occurred was partly cohesive and partly adhesive. The grooves (Fig. 13) resulted in very good anchoring of the deposit material and hence very often some chromium remained on the copper surface when the specimens were pulled apart.

4. Conclusions

Radio frequency plasma spraying constitutes an alternative processing technology to manufacture large chromium sputter

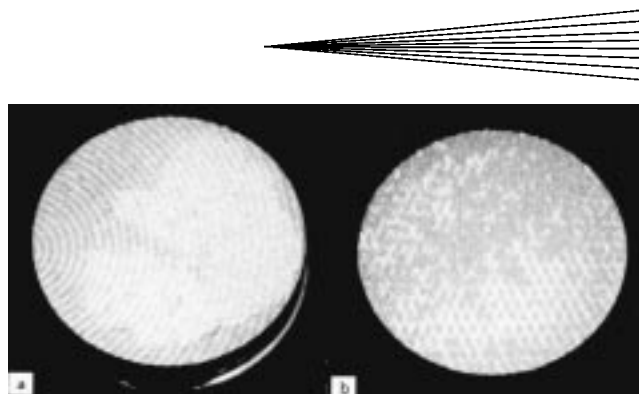


Fig. 13 The substrate side of tensile test specimens after adhesive (partly cohesive) failure during the tensile test. The failure load was 6.9 MPa (a), spiral pattern) and 8 MPa (b), diamond pattern)

targets. Powder feed rates of up to 80 g/min yielded good coating qualities for powder grain sizes of $-60 + 20 \mu\text{m}$. Using powder grain sizes of $-90 + 45 \mu\text{m}$, the feed rate is limited to below 60 g/min. Deposition efficiencies exceeding 80% can be easily achieved.

Direct water cooling of the substrates prevents any substrate bending. However, in this case, the adhesion strength of the chromium coating to the copper substrate is very low. Non-cooled substrates yielded the highest adhesion values. The bending of these noncooled substrates can be kept within acceptable limits and subsequently be corrected by machining, even though this additional production step compromises the overall economy of the fabrication process.

Good adhesion is also supported by a large surface area of the substrate, achieved in this case study by the application of a diamond pattern roughening treatment.

References

1. W. Kunert and A. Köhler: *VDI Berichte*, 1992, vol. 917, pp. 107-13 (in German).
2. K. Schwarz, W. Kunert, and A. Köhler: *DVS-Berichte*, 1996, vol. 175, pp. 170-73 (in German).
3. A. Köhler, W. Kunert, and K. Schwarz: *DVS-Berichte*, 1993, vol. 152, pp. 181-84 (in German).
4. H. Schumann: in *Metallographie*, 13th ed., Deutscher Verlag für Grundstoffindustrie, Leipzig, 1990.
5. M. Müller: Master's Thesis, Freiberg University of Mining and Technology, Freiberg, Germany, 1994 (in German).
6. Anon.: ASTM Designation C633—Standard Method of Test for Adhesive or Cohesive Strength of Flame-Sprayed Coatings, *19th Annual Book of ASTM Standards*, Part 17, ASTM, Philadelphia, PA, 1969, pp. 636-42.
7. Anon.: *European Norm: Testing of Thermally Sprayed Coatings—Determination of the Tensile Adhesion Strength*, EN 582, Comité Européen de Normalisation (CEN), 1993 (in German).
8. D.Y. Shih, C.-A. Chang, J. Paraszczak, S. Nunes, and J. Cataldo: *J. Appl. Phys.*, 1991, vol. 70 (6), pp. 3052-60.
9. M. Hansen: *Constitution of Binary Alloys*, 2nd ed., McGraw-Hill, New York, NY, 1958, p. 524.
10. R.P. Elliot: *Constitution of Binary Alloys*, 1st suppl., McGraw-Hill, New York, NY, 1965, p. 344.
11. D.J. Chakrabarti and D.E. Laughlin: in *Binary Alloy Phase Diagrams*, 2nd ed., T.B. Massalski, ed., ASM International, Materials Park, OH, 1990, p. 1267.